Highly efficient electro-optically *Q*-switched 473 nm blue laser

Tingting Lu (陆婷婷), Jian Ma (马 剑), Xiaolei Zhu (朱小磊)*, and Weibiao Chen (陈卫标)

Key Laboratory of Space Laser Communication and Detection Technology, Shanghai Institute of Optics and Fine Mechanics, Chinese Academy of Sciences, Shanghai 201800, China

**Corresponding author: xlzhu@siom.ac.cn*

Received December 28, 2018; accepted March 1, 2019; posted online May 17, 2019

An external frequency doubling electro-optically *Q*-switched neodymium-doped yttrium aluminum garnet (Nd:YAG) 473 nm blue laser was demonstrated. With absorbed pump energy of 48 mJ at 100 Hz repetition rate, about 2 mJ of 473 nm blue laser pulse energy was achieved by cascade frequency doubling. The second harmonic conversion efficiency was 64.5%, and overall optical-optical efficiency was 4.2%, respectively. The blue laser pulse width was less than 10 ns, and beam quality factor was less than 2.4.

OCIS codes: 140.3540, 140.3515, 140.3530, 140.3480.
doi: 10.3788/COL201917.051405.

Compact all-solid-state blue and green lasers have broad applications in ocean exploration systems, such as laser depth sounding, laser underwater communication, underwater target detecting, and seawater optical properties detecting, because of the especial seawater transmission window within the blue and green spectral bands[1]. Up to now, high peak power frequency doubled neodymium-doped solid-state green lasers, such as outputs at 532 nm[2–5], 526.5 nm[6–8], and 523.5 nm[9–11] wavelengths, have been greatly progressed and widely applied in marine scientific research. It has been proven that the green laser in the spectral range of 520–550 nm has higher transmission in coastal seawater, while the blue laser within the spectral range of 450–490 nm has higher transmission in deep seawater[12]. Therefore, the blue laser is more suitable for deep seawater exploration and has become a research hot-spot. As we know, frequency doubling from a 0.9 μm quasi-three-level transition of neodymium-doped laser gain medium is a common method to get a blue laser. In the past, many researchers focused on developing continuous-wave blue lasers[13–15], which are applicable for high-density optical data storage, flow cytometry, and color displays. But for applications of laser seawater depth sounding, laser underwater communication, and underwater target detection, high peak power and short pulse duration from an actively *Q*-switched blue laser will benefit the performance. Till now, there are a few reports on acousto-optically *Q*-switched blue lasers[16–19]. In 2015, Leeuwen *et al.* developed an acousto-optically *Q*-switched side-pumped frequency doubling neodymium-doped yttrium aluminum garnet (Nd:YAG) laser, producing 4.7 mJ, 473 nm blue laser pulse output at 170 Hz repetition rate, where the peak power was 174 kW, but the overall optical-optical efficiency was only 0.5%[20]. An electro-optically *Q*-switched blue laser can provide a narrow pulse as well as linearly polarized laser output. In 2015, Huang *et al.* reported a 1 kHz, 946 nm electro-optically *Q*-switched Nd:YAG laser. Maximum output power of 350 mW at 11 ns pulse duration was obtained with the absorbed pump power of 11.1 W; the corresponding peak power was 32 kW, and the optical-optical efficiency was 3.2%[21]. In 2018, Kornev *et al.* presented a 946 nm electro-optically cavity-dumping Nd:YAG laser. The output pulse energy of 2.5 mJ at 50 Hz with pulse width of 1.6 ns was obtained. The peak power was 1.6 MW, and the optical-optical efficiency was 3.9%[22]. However, as far as we know, no more works on frequency doubling electro-optically *Q*-switched 473 nm blue lasers have been reported.

In this Letter, we demonstrate a highly efficient electro-optically *Q*-switched external frequency doubling Nd:YAG blue laser. Approximately 2 mJ of 473 nm blue laser pulse was obtained at a repetition rate of 100 Hz. The pulse duration was about 10 ns, and the equivalent peak power was 0.2 MW. The second harmonic conversion efficiency was up to 64.5%, and overall optical-optical efficiency was more than 4.2%, which was much higher compared with previous works on acousto-optically *Q*-switched 473 nm blue lasers[16–20].

The schematic diagram of the electro-optically *Q*-switched external frequency doubling 473 nm blue laser is shown in Fig. 1. A linear laser resonator cavity with a geometric length of 145 mm was designed. One of the cavity mirrors was a concave mirror with a concave radius of 1000 mm. It was coated with high transmission at 808 nm and high reflectivity at 946 nm. The output coupler was coated with 60% reflectivity at 946 nm. In order to suppress the strong transition of $^4F_{3/2} \rightarrow {}^4I_{11/2}$

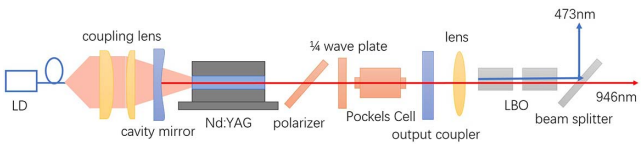

Fig. 1. Schematic diagram of the electro-optically *Q*-switched external frequency doubling 473 nm blue laser.

(emitting at 1064 nm), both cavity mirrors were coated with high transmission at 1064 nm.

The gain material was a composite YAG/Nd:YAG/YAG crystal rod with dimensions of $\phi 4$ mm × 40 mm. The dopant concentration was 0.3 at.%. Both end faces of the rod were coated with high-transmission films at 808, 946, and 1064 nm. The Nd:YAG rod was wrapped with indium foil and mounted in a water cooled heat sink made of red copper. The temperature of the heat sink was maintained at 17°C ± 0.5°C during the experiments.

A fiber-coupled 808 nm wavelength laser diode (nLIGHT Company, S0016-P6-110-0808-3-C-R02) with core diameter of 600 μm and numerical aperture of 0.22 was used as the pump source. In order to decrease the heat generation of the Nd:YAG crystal, which could dramatically influence the performance of quasi-three-level lasing, the pump diode was set to quasi-continuous-wave (QCW) operation. It was driven in a pulsed mode with a driven-pulse duration of 230 μs (FWHM) at a repetition rate of 100 Hz, equivalent to a duty cycle of 2.3%. The pump beam was coupled into the laser crystal by an optical transfer system. In the experiments, it was found that the pump power density in the laser crystal played an important role on influencing the output characteristic of 946 nm lasing. When the pump power density is relatively low, the laser output will be inefficient. In this design, the focal lengths of the coupling lens were chosen to be 40 and 60 mm, with corresponding magnification of 1.25, resulting in a 0.75 mm beam waist inside the Nd:YAG crystal. The absorption efficiency of the composite YAG/Nd:YAG/YAG crystal rod was about 96%. Moreover, a potassium dideuterium phosphate (KD*P) Pockels cell, a polarizing film, and a $\lambda/4$ wave plate were inserted in the resonator as an electro-optical Q switch.

The output characteristics of the 946 nm laser were first demonstrated without the external frequency doubling module. With the 40% output coupler at 946 nm, the output pulse energy as a function of the pump pulse energy in the long-pulse mode and Q-switched mode at 100 Hz repetition rate is shown in Fig. 2. As the absorbed pump energy was increased to 48 mJ, the maximum output energy of 5.7 mJ at 946 nm was obtained in the long-pulse mode. The relevant optical-optical conversion efficiency was 12%, and the slope efficiency was 20.6%. In the Q-switched mode, about 3.1 mJ pulse energy at 946 nm wavelength was achieved when the absorbed pump pulse energy reached up to 48 mJ. The optical-optical conversion efficiency was approximately 6.5% with respect to a slope efficiency of 10.8%, and higher pump energy input failed to obtain higher output due to the amplified spontaneous emission (ASE) of 1064 nm. The recorded spectrum of the Q-switched 946 nm laser is shown in Fig. 3, and no 1064 nm lasing was detected with the maximum output. Meanwhile, the beam quality of the 946 nm fundamental laser was measured by a Spiricon M^2-200 laser beam analyzer. The M^2 factors were measured as $M_x^2 = 1.4$ and $M_y^2 = 1.2$, as shown in Fig. 4. The difference of M^2 factors in the x and y directions was caused by the different stresses of the heat sink clamp in the two directions. The far-field beam profile of the 946 nm laser was also detected, which is shown in Fig. 5. The result indicates that the transverse electromagnetic (TEM_{00}) mode was achieved.

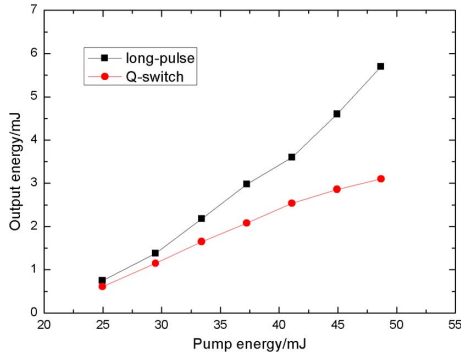

Fig. 2. Output energy of the 946 nm laser versus absorbed pump energy.

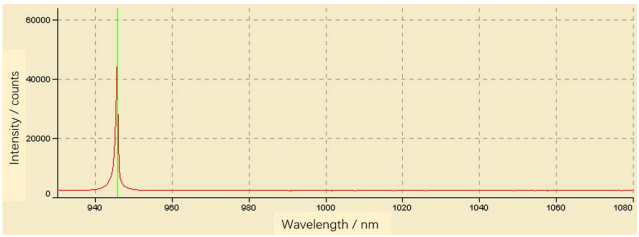

Fig. 3. Output spectrum of the 946 nm fundamental laser beam.

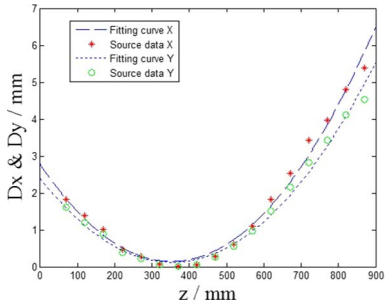

Fig. 4. Measurement of M^2 factors for the 946 nm laser.

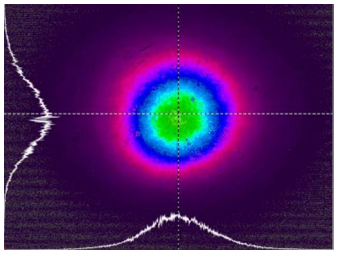

Fig. 5. Far-field beam profile of the 946 nm laser.

The second harmonic generation was realized by a type I phase matched lithium triborate (LBO) crystal. A beam splitter was placed behind the LBO crystal to split the 473 nm laser and the residual fundamental 946 nm laser. The LBO crystal was cut to 4 mm × 4 mm × 12 mm with phase matching angles of $\theta = 90°$ and $\phi = 19.3°$. The LBO was also wrapped with indium foil and mounted on a heat sink, and the temperature was controlled by a thermo-electric cooler with temperature accuracy of ±0.1°C. Both faces of the LBO were coated with high-transmission films at 946 and 473 nm wavelengths. The frequency doubling efficiencies of a single LBO crystal and cascade double LBO crystals were compared in the experiments. At the repetition frequency of 100 Hz, when the absorbed pump pulse energy was 48 mJ, the 473 nm laser pulse energy was scaled up to 1.4 mJ for single LBO. The frequency doubling conversion efficiency was 45.1%. The overall optical to optical conversion efficiency was 2.9%, and the slope efficiency was 6.1%. For the cascade double LBO arrangement, the output energy of the 473 nm laser was increased up to 2 mJ with a pulse width of less than 10 ns, the frequency doubling conversion efficiency was 64.5% with overall optical to optical conversion efficiency of 4.2%, and the slope efficiency reached up to 8.3%. The output 473 nm pulse energy as a function of the pump pulse energy for single LBO and double LBO is shown in Fig. 6. Higher second harmonic conversion efficiency was obtained by the cascade double LBO arrangement. The pulse waveform and pulse train recorded by an oscilloscope (Tektronix MDO4034 C) are shown in Figs. 7 and 8. Figure 9 shows the far-field beam profile of the blue laser measured by a CCD camera (Spiricon, SP620) at maximum pulse energy. The beam profile shows the blue laser was still in the TEM_{00} mode. The beam parameter product (BPP) at maximum output energy in both the x and y directions was measured by the CCD camera. According to the M^2-factor definition, $M^2 = (\omega\theta)/(\omega_0\theta_0) = \mathrm{BPP}/(2\lambda/\pi)$[23]; the M^2-factors of blue laser were calculated to be $M_x^2 = 2.4$ and $M_y^2 = 2.3$. The output spectrum of the blue laser was measured by an optical spectrum analyzer (Yokogawa AQ6374). As shown in Fig. 10, the central wavelength was measured to be 473.1 nm.

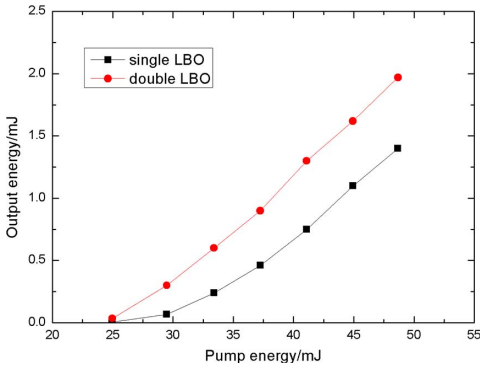

Fig. 6. Output energy of the 473 nm laser as a function of 808 nm pump energy.

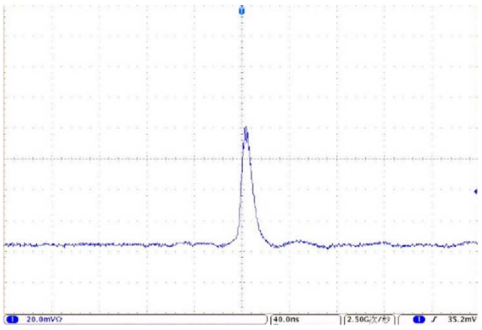

Fig. 7. Pulse waveform of the 473 nm laser.

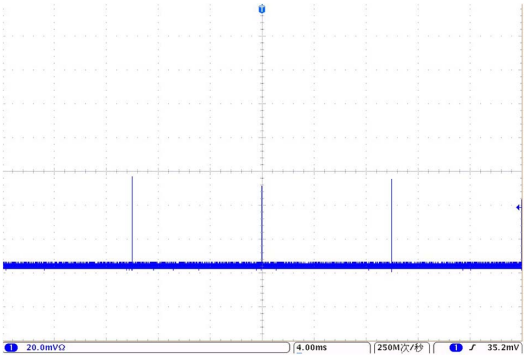

Fig. 8. Pulse train of the 473 nm laser.

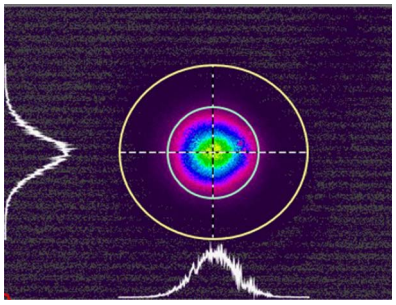

Fig. 9. Far-field beam profile of the blue laser.

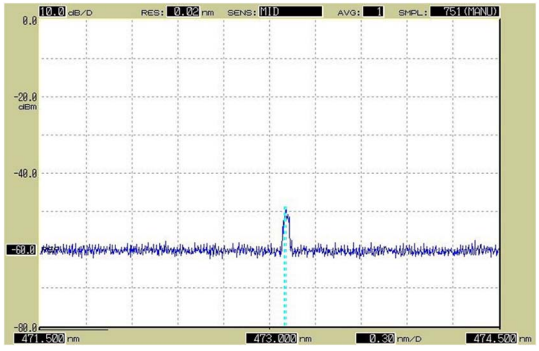

Fig. 10. Output spectrum of the blue laser.

In conclusion, we have demonstrated a laser-diode end-pumped, external frequency doubling, electro-optically Q-switched Nd:YAG blue laser emitting at 473 nm. This blue laser succeeded in generating 2 mJ pulse energy in

the TEM_{00} mode with a pulse width of 10 ns at the repetition rate of 100 Hz. The equivalent peak power was 0.2 MW, and the overall optical-optical efficiency was 4.2%. The blue laser beam quality factors were measured as $M_x^2 = 2.4$ and $M_y^2 = 2.3$. Such a compact high peak power 473 nm TEM_{00} mode laser with comparatively high efficiency can be widely used in oceanic applications.

This work was supported by the National Key Research and Development Program of China (No. 2016YFC1400902).

References

1. S. A. Sullivan, J. Opt. Soc. Am. A **53**, 962 (1963).
2. H. Zhang, X. Liu, D. Li, P. Shi, A. Schell, C. R. Haas, and K. Du, Appl. Opt. **46**, 6539 (2007).
3. Z. Zhang, Q. Liu, and M. Gong, Appl. Opt. **52**, 2735 (2013).
4. Q. Zheng, L. Zhao, Z. Ye, H. Tan, and L. Qian, Opt. Laser Technol. **33**, 355 (2001).
5. T. Lu, J. Wang, X. Zhu, R. Zhu, H. Zang, and W. Chen, Chin. Opt. Lett. **11**, 051402 (2013).
6. X. Peng, L. Xu, and A. Asundi, Appl. Opt. **44**, 800 (2005).
7. Y. B. Zhang, Y. X. Zheng, Y. H. Jia, and Y. Yao, Laser Phys. **20**, 1580 (2010).
8. T. Lu, J. Wang, M. Huang, D. Liu, and X. Zhu, Chin. Opt. Lett. **10**, 081403 (2012).
9. T. Lu, J. Ma, M. Huang, Q. Yang, X. Zhu, and W. Chen, Chin. Phys. Lett. **31**, 074208 (2014).
10. D. Li, Z. Ma, P. Loosen, and K. Du, Opt. Lett. **32**, 1272 (2007).
11. Q. Yang, X. Zhu, J. Ma, T. Lu, X. Ma, and W. Chen, Opt. Commun. **354**, 414 (2015).
12. G. D. Ferguson, Proc. SPIE **0064**, 150 (1975).
13. S. Bjurshagen, D. Evekull, and R. Koch, Appl. Phys. B **76**, 135 (2003).
14. C. Czeranowsky, E. Heumann, and G. Huber, Opt. Lett. **28**, 432 (2003).
15. Y. Chen, H. Peng, W. Hou, Q. Peng, A. Geng, L. Guo, D. Cui, and Z. Xu, Appl. Phys. B **83**, 241 (2006).
16. F. Chen, X. Yu, R. Yan, X. Li, C. Wang, J. Yu, and Z. Zhang, Opt. Lett. **35**, 2714 (2010).
17. Y. Chen, W. Hou, H. Peng, H. Zhang, L. Guo, H. Zhang, D. Cui, and Z. Xu, Opt. Commun. **270**, 58 (2007).
18. J. Gao, X. Yu, X. Li, F. Chen, Z. Zhang, J. Yu, and Y. Wang, Laser Phys. Lett. **5**, 433 (2008).
19. F. Chen, X. Yu, K. Zhang, Y. He, C. Zheng, C. Wang, and J. Guo, J. Opt. Laser Technol. **68**, 36 (2015).
20. R. Van Leeuwen, T. Chen, L. Watkins, G. Y. Xu, J. F. Seurin, Q. Wang, D. L. Zhou, and C. Ghosh, Proc. SPIE **9342**, 93420N (2015).
21. J. Huang, X. Hu, and W. Chen, Chin. Opt. Lett. **13**, 021402 (2015).
22. A. F. Kornev, V. P. Pokrovskiy, S. V. Gagarskiy, Y. Y. Fomicheva, P. A. Gnatyuk, and A. S. Kovyarov, Opt. Lett. **14**, 43 (2018).
23. B. Zhou, Y. Gao, Z. Chen, and J. Chen, *Laser Principles* (National Defense Industry Press, 2008).